Non-equilibrium dynamics of Bosonic Mott insulators in an electric field

M. Kolodrubetz[1], D. Pekker[2], B. K. Clark[1,3], and K. Sengupta[4]
[1] *Department of Physics, Princeton University, Princeton, NJ 08544, USA.*
[2] *Department of Physics, California Institute of Technology, Pasadena, CA 91125, USA.*
[3] *Princeton Center for Theoretical Science, Princeton University, Princeton, NJ 08544, USA.*
[4] *Theoretical Physics Department, Indian Association for the Cultivation of Science, Jadavpur, Kolkata-700032, India.*
(Dated: June 22, 2011)

We study the non-equilibrium dynamics of one-dimensional Mott insulating bosons in the presence of a tunable effective electric field $\mathcal{E}$ which takes the system across a quantum critical point (QCP) separating a disordered and a translation symmetry broken ordered phase. We provide an exact numerical computation of the residual energy Q, the log-fidelity F, the excess defect density D, and the order parameter correlation function for a linear-in-time variation of $\mathcal{E}$ with a rate v. We discuss the temporal and spatial variation of these quantities for a range of v and for finite system sizes as relevant to realistic experimental setups [J. Simon *et al.*, Nature **472**, 307 (2011)]. We show that in finite-sized systems Q, F, and D obey Kibble-Zurek scaling, and suggest further experiments within this setup to test our theory.

PACS numbers: 75.10.Jm, 73.43.Nq

Ultracold atoms in optical lattices provide us with a unique opportunity to study both equilibrium phases and non-equilibrium quantum dynamics of strongly coupled bosonic systems near a quantum phase transition (QPT) [1]. One system, which has been the subject of a recent experimental study, consists of one-dimensional (1D) Mott insulating (MI) bosons in the presence of an effective electric field $\mathcal{E}$ [2]. It has been shown that this system can be described in terms of an effective quantum dipole model or, equivalently, an Ising spin model with infinitely strong nearest neighbor coupling in the presence of both a transverse and a longitudinal field [3]. It has also been demonstrated in Ref. [3], that tuning $\mathcal{E}$ to a critical value $\mathcal{E}_c$ leads to a QPT. In the dipole language, this transition consists of a change in the ground state from a dipole vacuum (which corresponds to $\bar{n}$ bosons at each site) to one with maximal dipoles (which corresponds to alternating $\bar{n}-1$ and $\bar{n}+1$ bosons per site). In the spin language, this transition is from the paramagnet (PM) to an Ising antiferromagnet (AFM). The intermediate QCP belongs to the Ising universality class [3]. The appearance of this AFM order has recently been observed using a quantum gas microscope [2]. Theoretical studies of the phases of the bosonic Mott insulator in an electric field have also been extended to several 2D lattices [4].

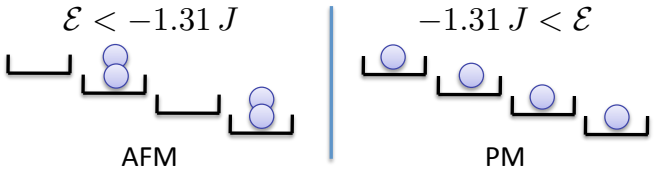

FIG. 1: (color online) A pictorial representation of the dipole (AFM) and the vacuum (PM) ground states for MI bosons with $\bar{n} = 1$ across the quantum phase transition. The transition occurs at $U - \mathcal{E}_c = -1.31$ (for $J = 1$).

The study of non-equilibrium dynamics of closed quantum systems have seen tremendous progress in recent years [5]. One reason for this intense effort has been the possibility of experimentally realizing these dynamics using ultracold atoms. Indeed, experiments probing non-equilibrium phenomena with strongly coupled 2D bosonic atoms, well described by the 2D Bose-Hubbard model, have been carried out recently [6]. The corresponding theoretical studies show a reasonable qualitative match with experiments [7]. For the case of 1D bosonic MI in the presence of an electric field, order parameter dynamics following sudden quenches of the electric field have also been studied theoretically [8]. However, the case of finite velocity and, in particular, nearly adiabatic ramps of $\mathcal{E}$ has not been previously explored.

In this letter, we probe the non-equilibrium dynamics of the bosonic Mott insulators in the presence of a linear-in-time varying electric field (chemical potential gradient)

$$\mathcal{E}(t) = \mathcal{E}_i + (\mathcal{E}_f - \mathcal{E}_i)t/\tau, \tag{1}$$

where $\mathcal{E}_i$ and $\mathcal{E}_f$ are the initial and final values of the electric field, and τ is the ramp time. We define the ramp rate to be $v = \partial_t \mathcal{E}(t)$. We look at ramps that start from the PM phase with unit boson occupation per site and end either in the AFM phase across the QPT or at the QCP. Based on the resonant manifold model of Ref. [3], we provide an exact numerical computation for finite system sizes (L), using Exact Diagonalization (ED, $L \leq 16$) and time dependent Matrix Product States (tMPS, $L \leq 48$), of the residual energy Q, the log-fidelity F, the number of defects D (a defect, for the ramps we address, is a doubly occupied or empty lattice site), and the defect correlation function $C_{ij}(t)$. We note that the experimental setup of Ref. [2] constitutes systems of $L \leq 16$ lattice sites and measures D as well as $C_{ij}(t)$; hence our theoretical analysis constitutes

a quantitatively exact description of the dynamics of the experimental system providing a valuable guideline to future experiments. Further, for finite sized systems, our analysis reveals the manifestation of universal Kibble-Zurek-like (KZ) scaling [9–11]. In the past, KZ scaling has been shown to work well in integrable systems [12]; however, its manifestation in non-integrable systems has not been consistently demonstrated [13]. Our work thus provides the first realization of KZ scaling in finite-sized non-integrable systems which can be tested with an existing experimental setup. Furthermore, we investigate the crossover from Landau-Zener (LZ) scaling [10, 14] to KZ scaling in finite-size systems, and show that it collapses onto a universal functional form, as suggested in Ref. [15].

Model — Bosonic atoms in a tilted optical lattice (i.e. in an effective time dependent electric field) are well described using the Bose-Hubbard Hamiltonian [3]

$$H_B(t) = -t_0 \sum_{\langle ij \rangle} b_i^\dagger b_j + \frac{U}{2} \sum_i n_i(n_i - 1) - \mathcal{E}(t) \sum_i i \cdot n_i$$

where $\langle ij \rangle$ denotes the sum over nearest-neighbors, b_i the boson annihilation operator at site i, and $n_i = b_i^\dagger b_i$ the boson density operator. Under the condition $U, \mathcal{E}(t) \gg |U - \mathcal{E}(t)|, t_0$, the low-energy dynamics of H_B are captured by an effective dipole model [3]

$$H_d(t) \;=\; [U - \mathcal{E}(t)] \sum_\ell d_\ell^\dagger d_\ell - J \sum_\ell (d_\ell^\dagger + d_\ell), \quad (2)$$

where $d_\ell = b_i b_j^\dagger / \sqrt{n_0(n_0+1)}$ denotes the dipole annihilation operator which lives on a link ℓ between the neighboring sites i and j as schematically shown in Fig. 1, n_0 the boson occupation of parent Mott insulator, and $J = t_0\sqrt{n_0(n_0+1)}$ the amplitude for creation or annihilation of a dipole. Henceforth, we shall use the units in which $\hbar = 1$, $J = 1$, and restrict ourselves to $n_0 = 1$. The dipoles satisfy two constraints; first, there can be only one dipole on any link ℓ which renders $d_\ell^\dagger d_\ell \leq 1$, and second, two consecutive links can not be simultaneously occupied by dipoles $d_\ell^\dagger d_{\ell+1}^\dagger d_{\ell+1} d_\ell = 0$. These constraints render H_d non-integrable; however, they also lead to a significant reduction in the Hilbert space of H_d which makes ED and tMPS the methods of choice for studying the dynamics of the model. In addition, we restrict ourselves to studying H_d with periodic boundary conditions so as to approach the thermodynamic limit with smaller systems. We note that the dipole model can be represented in terms of an Ising-like spin-model via the transformation: $S_\ell^z = 1/2 - d_\ell^\dagger d_\ell$, $S_\ell^{x(y)} = (-i)(d_\ell + (-)d_\ell^\dagger)/2$ [2, 3]. Note that $\langle S_\ell^z \rangle$ is the order parameter for the transition from the PM (dipole vacuum) to the AFM (maximal dipole density) state.

To study the dynamics within exact diagonalization, we evolve the wave function using the time dependent Hamiltonian of Eq. (2), in which the electric field is tuned linearly in time according to Eq. (1)

$$i\hbar\partial_t |\psi(t)\rangle = H_d(t)|\psi(t)\rangle. \quad (3)$$

We supplement the time evolution with the initial condition $|\psi(t=0)\rangle = |\psi_G\rangle_i$, where $|\psi_G\rangle_i$ is the ground state wave function of the initial Hamiltonian. Integrating Eq. (3) from $t = 0$ to $t = \tau$ we obtain the wave function at the end of the ramp $|\psi(\tau)\rangle$.

We supplement our exact diagonalization studies by tMPS, which allows us to study larger system sizes. tMPS represents the wave function as $|\psi\rangle = \sum_{\{\sigma_i\}} M_1^{\sigma_1} M_2^{\sigma_2} ... M_L^{\sigma_L} |\sigma_1, \sigma_2 ...\rangle$, where $M_i^{\sigma_i}$ are a set of χ by χ matrices indexed by site i and spin σ_i [16]. We take advantage of the fact that in the reduced Hilbert space the Hamiltonian $H_d(t)$, Eq. (2), is a sum of single site Hamiltonians to perform time evolution. We evolve in time via $|\psi(t+\epsilon)\rangle = P \exp(-i\epsilon H_d(t))$ by first exactly applying the single site hamiltonian $H_d(t)$ and then projecting out configurations with neighboring dipoles using the projection operator P. This projection increases the MPS bond dimension which is then reduced back to its original value χ introducing a small error. The method becomes exact in the limit $\epsilon \to 0$ and matrix size $\chi \to \infty$, and its convergence has been numerically checked by extrapolating in these parameters [17]. Ground states are found by evolving the same Hamiltonian to large imaginary time at fixed $\mathcal{E}$.

For this work, the specific observables of interest will be the residual energy Q, the log-fidelity F, the defect number n_d (i.e. the number of sites with even parity of the boson occupation number), excess defect number D, and the spin-spin correlation function C_{ij} which, at any instant t, are given by

$$Q(t) = \langle\psi(t)|H(t)|\psi(t)\rangle - E_G(t), \quad (4)$$

$$F(t) = \log[|\langle\psi(t)|\psi_G(t)\rangle|^2], \quad (5)$$

$$n_d(t) = \langle\psi(t)|\sum\nolimits_\ell (1 + 2S_\ell^z)\,|\psi(t)\rangle, \quad (6)$$

$$D(t) = n_d(t) - \langle\psi_G(t)|\sum\nolimits_\ell (1 + 2S_\ell^z)\,|\psi_G(t)\rangle, \quad (7)$$

$$C_{ij}(t) = \langle\psi(t)|S_i^z S_j^z|\psi(t)\rangle, \quad (8)$$

where $E_G(t)$ $[|\psi_G(t)\rangle]$ corresponds to the ground state energy [wave function] of the Hamiltonian $H_d(t)$. For notational brevity, we shall drop the index t from observables when evaluating them at the end of the ramp ($t = \tau$).

We begin with a discussion of Q and F for finite size systems ($L \leq 48$) undergoing ramps from the PM phase ($U - \mathcal{E}_i = 100$) to the QCP ($U - \mathcal{E}_f = U - \mathcal{E}_c = -1.31$) in time τ. For a finite size system which is always gapped, Q and F behave differently than their counterparts in the thermodynamic limit ($L \to \infty$) for which one expects KZ-like scaling to manifest in both $Q \sim v^{(d+z)\nu/(z\nu+1)}$ and $F \sim v^{d\nu/(z\nu+1)}$ for small v (large τ). Here $d = 1$ is

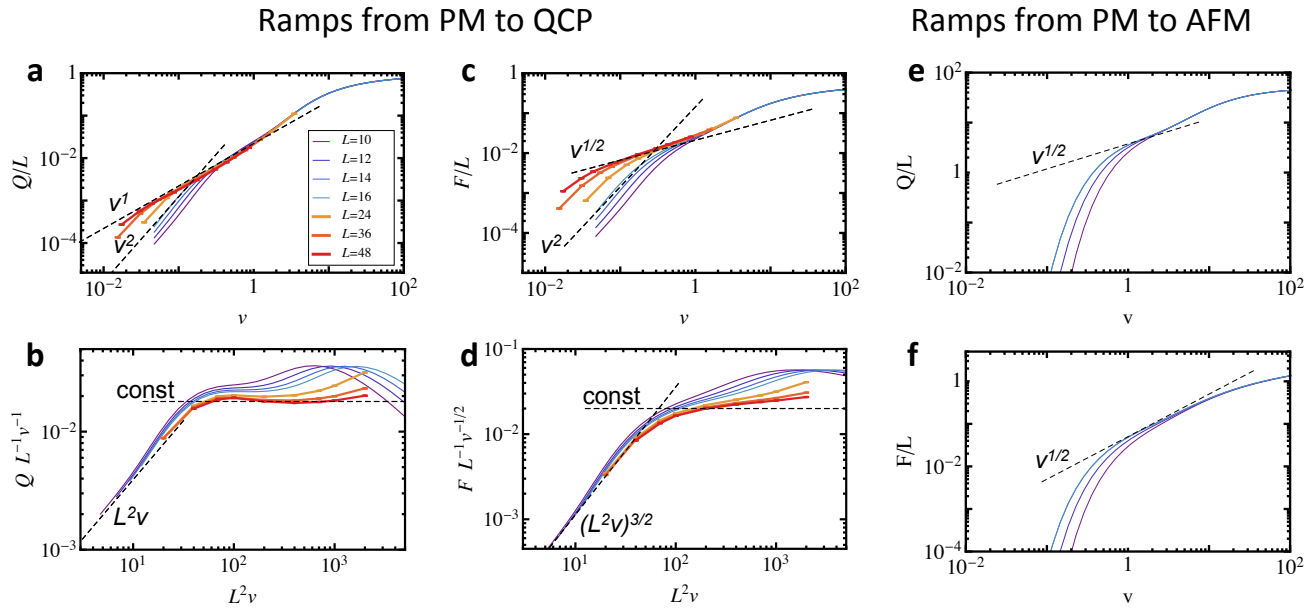

FIG. 2: (color online) Residual energy Q (a) and log-fidelity F (c) as a function of the ramp rate $v = \partial_t \mathcal{E}(t)$ for various system sizes from $10 \leq L \leq 16$ (ED) and $24 \leq L \leq 48$ (tMPS, error bars correspond to time step extrapolation error, bond dimension errors are below 10^{-4}). The ramps start in the PM ($U - \mathcal{E}_i = 100$) and end at the QCP ($U - \mathcal{E}_f = -1.31$). Dashed lines show the indicated power laws. Note the extension of the intermediate Kibble-Zurek-like scaling regime to lower values of v for larger system sizes. (b) and (d) show finite size scaling collapse for Q and F for several L. (e) and (f) show Q and F as a function of v for ramps starting in the PM ($U - \mathcal{E}_i = 100$) and ending in the AFM phase ($U - \mathcal{E}_f = -100$) with $10 \leq L \leq 14$. Note the change in Q power law from v^1 to $v^{1/2}$.

the dimensionality, $z = 1$ is the dynamical critical exponent, and $\nu = 1$ the correlation length critical exponent. For very fast ramps, the wave function does not have time to evolve during the dynamics, and therefore the behavior of finite- and infinite-sized systems is similar but not universal. As the ramp rate becomes slower ($v \sim 1$), KZ scaling sets in for both infinite- and finite-sized systems. However, while KZ scaling is expected to persist to infinitely slow ramps in the thermodynamic limit, for finite-sized systems it is cut off for ramps slower than a critical ramp rate $v_c(L) \sim L^{-(1/\nu+z)}$. For $v \leq v_c(L)$, Q and F are expected to scale as v^2 as in gapped systems [10, 14]. These expectations may be formalized in the form of scaling functions

$$Q \sim L^d v^{(d+z)\nu/(z\nu+1)} g_r(vL^{1/\nu+z}), \quad (9)$$

$$F \sim L^d v^{d\nu/(z\nu+1)} f_r(vL^{1/\nu+z}), \quad (10)$$

where $g_r(x \ll 1) \sim x^{2-(d+z)\nu/(z\nu+1)}$, $f_r(x \ll 1) \sim x^{2-d\nu/(z\nu+1)}$ (very slow, i.e. LZ regime) and $g_r(x \gg 1) \sim$ const., $f_r(x \gg 1) \sim$ const. (KZ regime) [15].

The above-mentioned expectations are corroborated in panels (a) and (c) of Fig. 2, which show the behavior of Q and F as a function of the quench rate v^1 for several system sizes $10 \leq L \leq 48$ on a log-log scale. For both Q and F we find v^2 scaling for very slow ramps and KZ-like scaling $Q \sim v^1$ and $F \sim v^{1/2}$ for intermediate ramps. Finally, for fast ramps, we find non power-law behavior followed by a plateau. We note that KZ-like scaling only occurs in systems of sufficient size ($L \geq 10$ for Q and $L \geq 16$ for F) [18]. The LZ-KZ scaling crossover (Eqs. (9) and (10)) is further corroborated in panels (b) and (d) of Fig. 2. These plots demonstrate both the scaling collapse of Q and F for slower ramps (points to the left) and their deviations from scaling for faster ramps (points to the right) in the non-universal regime. The dashed lines indicate the expected form of the scaling functions g_r and f_r in both the LZ and the KZ regimes. Note that for the LZ regime, we see collapse even for relatively small system sizes ($L \gtrsim 10$); however, for the KZ regime collapse only occurs for larger system sizes ($L \gtrsim 16$ for Q and $L \gtrsim 48$ for F).

Next, we study ramps that cross the QCP. As the system progresses towards the QCP, the gap closes, and excitations are produced. At some later time, after passing the QCP, the gap reopens, and no new excitations can be created. However, although the number of excitations is conserved in the final adiabatic part of the ramp, the energies of individual excitations continue changing. Therefore, in ramps across the QCP, we can expect to see KZ-like scaling for F but not for Q. These expectations are corroborated in panels (e) and (f) of Fig. 2, in which we plot Q and F as a function of the ramp rate v^1 for ramps from PM ($U - \mathcal{E}_i = 100$) to AFM phase ($U - \mathcal{E}_f = -100$). We find KZ-like scaling in $F \sim v^{1/2}$ as

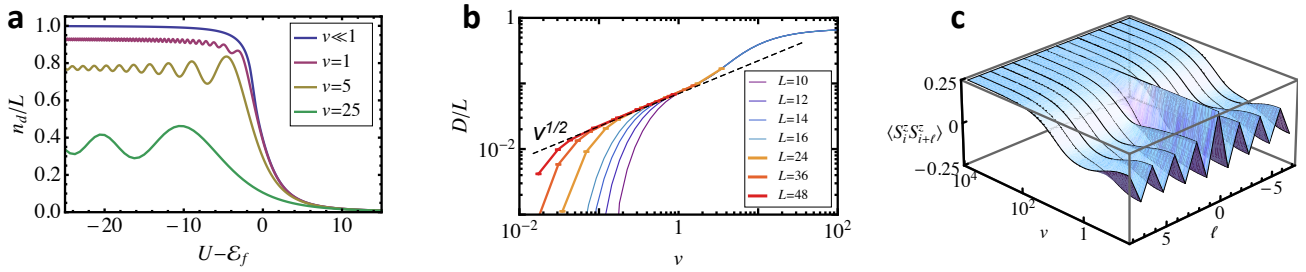

FIG. 3: (color online) (a) n_d/L as a function of the end point of the ramp $U-\mathcal{E}_f$ for several ramp rates (all ramps start in the PM phase $U-\mathcal{E}_i=50$). (b) D as a function of v for several L showing KZ scaling ($U-\mathcal{E}_i=100$, $U-\mathcal{E}_f=-1.31$). (c) Spin-spin correlation function $C_\ell=\langle S_i^z S_{i+\ell}^z\rangle$ at the end of the ramp as a function ℓ and the ramp rate v for $L=16$.

expected; interestingly Q also scales as $v^{1/2}$. This happens due to the fact that during the adiabatic part of the ramp, almost all excitations are converted into singly occupied sites, with energy per excitation of $\sim|U-\mathcal{E}_f|$. Therefore Q becomes identical to the number of excitation and hence scales in the same way as F. Thus our analysis suggest anomalous scaling of Q in ramps across the QCP should be interpreted with caution.

Having obtained the scaling behavior, we concentrate on its manifestation for experimentally observable quantities. We note that the existing experimental setup [6] focuses on imaging the parity of the number of bosons on each site, after projecting the wave function into a Fock state [1, 2, 6]. Effectively, this imaging counts the number of empty and doubly occupied sites (i.e. "defects" on the PM side). In addition to measuring this defect number n_d, the existing experiments can measure the defect-defect correlation function $g_d(\ell)=\langle n_d(i)n_d(i+\ell)\rangle\sim\langle S_i^z S_{i+\ell}^z\rangle=C_{i,i+\ell}$ at the end of the ramp. In Fig. 3a, we plot the defect density n_d as a function of the $U-\mathcal{E}_F$. We note that the final saturation value of n_d in the AFM phase is a decreasing function of the ramp rate and lies between those for a nearly adiabatic ramp and a sudden quench. In Fig. 3b, we show that the excess defect number D demonstrates similar finite-size KZ scaling as F. Since n_d is experimentally measurable, our work demonstrates that finite size scaling can be observed within an existing experimental setup. Finally, in Fig. 3c, we show the behavior of $C_{i,i+\ell}$ as a function of v and ℓ. We note that for slow ramps to the QCP one finds an oscillatory behavior of $C_{i,i+\ell}$ indicating the precursor of the AFM order present in the critical ground state. As v is increased, the system ceases to reach the final ground state and these correlations decay. Finally, the state of the system at the end of fast ramps is essentially the PM ground state, which has no AFM correlations, leading to a flat $C_{i,i+\ell}$. These features can be directly picked up in experiments, which can serve as a test of our theory.

In conclusion, we have investigated universal scaling dynamics of finite size non-integrable bosonic system following a finite rate ramp of the effective electric field. Our investigation demonstrates two scaling regimes (LZ- and KZ-like scaling) with conventional exponents and thus differ from prior studies of other non-integrable systems [9, 12, 13] which found various anomalous scaling exponents. Furthermore, comparing ramps that cross the QCP (which show anomalous exponents) to those that end at the QCP (which show expected exponents), we suggest a possible origin of these anomalous exponents: the adiabatic dynamics of the excitations following the passage through the quantum critical regime. Finally, we compute experimentally measurable quantities such as n_d and C_{ij} and demonstrate that the scaling behavior studied in this work can be observed in realistic experiments via measurement of n_d.

It is our pleasure to thank A. Polkovnikov for invaluable discussions. We acknowledge support from the Lee A DuBridge fellowship (DP), IIAS, PCTS. KS thanks DST, India for support through grant SR/S2/CMP-001/2009. DP and BKC thank the Aspen Center for Physics for its hospitality.

[1] M. Greiner *et al.*, Nature (London) **415**, 39 (2002).
[2] J. Simon *et al.*, Nature **472**, 307 (2011).
[3] S. Sachdev, K. Sengupta, and S. M. Girvin, Phys. Rev. B **66**, 075128 (2002).
[4] S. Pielawa *et al.* Phys. Rev. B **83**, 205135 (2011)
[5] A. Polkovnikov *et al.*, arXiv:1007.5331; D. Ziarmaga, Adv. Phys. **59**, 1063 (2010).
[6] W. Bakr *et al.*, Science **329**, 547 (2010).
[7] C. Trefzger and K. Sengupta Phys. Rev. Lett. **106** 095702 (2010).
[8] K. Sengupta, S. Powell, and S. Sachdev, Phys. Rev. A **69**, 053616 (2004).
[9] T. W. B. Kibble, J. Phys. A **9**, 1387 (1976); W. H. Zurek, Nature **317**, 505 (1985);
[10] A. Polkovnikov and V. Gritsev, Nat. Phys. **4**, 477 (2008). C. De Grandi and A. Polkovnikov, "Quantum Quenching, Annealing and Computation," Eds. A. Das, A. Chandra, and B. K. Chakrabati, Lect. Notes in Phys., vol. 802 (Springer, Heidelberg 2010).
[11] M. M. Rams and B. Damski, Phys. Rev. Lett. **103**. 170501 (2009).
[12] A. Polkovnikov, Phys. Rev. B **72**, 161201(R) (2005); R.

W. Cherng and L. S. Levitov, Phys. Rev. A **73**, 043614 (2006); C. De Grandi, V. Gritsev, and A. Polkovnikov, Phys. Rev. B **81**, 224301 (2010).

[13] F. Pollmann, S. Mukerjee, A. G. Green, and J. E. Moore, Phys. Rev. E **81**, 020101(R) (2010); J.-S. Bernier, G. Roux, C. Kollath, arXiv:1010.5251.

[14] N. Vitanov and B. M. Garraway, Phys. Rev. A **53**, 4288 (1996).

[15] C. de Grandi, A. Polkovnikov, and A. Sandvik, arXiv:1106.XXXX (2011).

[16] U. Schollwock, Ann. Phys. **326**, 96 (2011); G. Vidal, Phys. Rev. Lett. **91**, 147902 (2003).

[17] To speed up tMPS, for slower ramp rates we move the starting point $U - \mathcal{E}_i$ closer to the QCP. We have verified this does not affect the observables.

[18] Care must be taken in interpreting data on smaller systems, as these appear to show a small segment of anomalous power-law like scaling in the KZ regime. However, this behavior is a finite size effect and the universal KZ exponents are restored for larger system sizes.